doi: 10.32131/jes.2.11

Journal of the Earth Simulator, Volume 2, March 2005, 11–33

Numerical Approach for Noise Reduction of Wind Turbine Blade Tip with Earth Simulator

Chuichi Arakawa*[1], Oliver Fleig[1], Makoto Iida[1] and Masakazu Shimooka[1]

[1] *Department of Mechanical Engineering, Interfaculty Initiative in Information Studies, The University of Tokyo, Hongo, Bunkyo-Ku, Tokyo 113-8656, Japan.*

(Received February 14, 2005; Revised manuscript accepted Mach 1, 2005)

Abstract The purpose of this research is to investigate the physical mechanisms associated with tip vortex noise caused by rotating wind turbines with giant size of computational fluid dynamics. The flow and acoustic field around the WINDMELIII wind turbine is simulated using compressible Large-Eddy simulation (LES), with emphasis on the blade tip region. The acoustic near field is simulated directly by LES whereas the far field is modeled using acoustic analogy. Due to the fine grid employed, smallest eddy scales near the blade surface are resolved. Aerodynamic performance and acoustic emissions are predicted for the actual tip shape and an ogee type tip shape. A decrease of the sound pressure level in the high frequency domain is observed for the ogee type tip shape. The present simulation research using the Earth Simulator shows that large scale simulation is really useful in designing the aerodynamic manufacturing such as the wind turbine.

Keywords: Wind Turbine, Large-Eddy Simulation, Noise, Earth Simulator.

1. Introduction

1.1 Background of research

There is a strong need to predict aerodynamic noise emitted by wind turbines and to find noise reducing design concepts in order to increase public acceptance of wind energy. Wind turbine blade manufacturers are interested in small modifications of a given blade geometry and its exact influence on the aerodynamic noise. Empirical models have been developed to predict the overall noise emitted by a wind turbine. However, current empirical models do not contain an accurate description of the wind turbine blade geometry and its relations to emitted noise. It is therefore necessary to develop models that take the correct blade geometry into account in order to design new blades with respect to noise reduction. CFD (Computational Fluid Dynamics) has become a useful tool to numerically simulate the complex flow and aerodynamic noise for engineering applications. However, CFD still remains computationally expensive regarding large-scale simulation of a full wind turbine including noise prediction. Through recent advances in computational power such as the development of the Earth Simulator we have come a step closer to large-scale numerical simulations.

1.2 Wind turbine noise

Wind turbines in operation emit noise that is a major problem for the public acceptance of wind energy. There is a strong need to develop noise prediction methods and to find noise reducing concepts for wind turbines to be able to further expand wind turbine sites. Wind turbine noise has aerodynamic and mechanical origins. Mechanical noise is caused by gears and bearings. Mechanical noise has been reduced considerably over the past years and is becoming less of a concern. It can be kept within limits by proper insulation around the gearbox. To further reduce wind turbine noise, focus must be placed on aerodynamic noise.

Different types of aerodynamic noise can be distinguished, notably low frequency noise and high frequency broadband noise, as described in Burton et al. [1]. Noise emitted by wind turbines can have a significant impact on the population residing near the wind turbines. The installation of wind turbines is becoming a serious problem in countries with high population density as a result of wind turbines producing aerodynamic noise. The noise of wind turbines is a major problem for the public acceptance of wind energy. Noise is becoming a serious concern early in the design process rather than a problem to be corrected during the production or testing stages.

* ***Corresponding author***: *Dr. Chuichi Arakawa, Department of Mechanical Engineering, Interfaculty Initiative in Information Studies, The University of Tokyo, 7-3-1 Hongo, Bunkyo-Ku, Tokyo 113-8656, Japan. E-mail: arakawa@cfdl.t.u-tokyo.ac.jp*

Tip vortex noise forms an important part of the noise generation process on the outer part of the wind turbine blades. Blade tip noise is caused by the three dimensional tip effects, possibly as the result of the turbulence in the locally separated flow region associated with the formation of the cross flow around the tip edge and the formation of the tip vortex and by instabilities in the viscous shear layer between the vortex and free stream (Wagner et al., [2]). The turbulent flow is convected inboard and aft towards the trailing edge, and noise might be caused as a result of the interaction of the tip vortex and the trailing edge. However, the exact mechanisms of blade tip noise generation have not been fully understood.

Brooks and Marcolini [3] experimentally investigated tip vortex noise formation for rectangular planform and rounded tips. They found that for the stationary blades, tip vortex noise is of lesser importance to the overall broadband self-noise spectrum than boundary layer and trailing edge noise. However, they mention that this necessarily will not be so for rotor systems because of the tip's relatively higher velocities compared to the inboard regions of the blade and the tip loading which should be high. They recommend including the tip noise in the overall noise spectrum prediction to obtain accurate noise spectra.

The importance of noise emission in the outer blade region was also pointed out by Nii et al. [4]. They performed acoustic tests on the WINDMELIII, shown in Fig. 1. WINDMELIII was developed at the National Institute of Advanced Industrial Science and Technology. A noise source was found to be located at the very tip of the blade for frequencies from 3.1 kHz to 6.3 kHz, suggesting a small but intense vortex shedding from the tip. As a general conclusion of the acoustic tests on WINDMELIII, the authors state that highest levels of noise source were found to be in the blade tip region, with levels decreasing towards the blade root.

The above-mentioned facts make clear that the study of noise caused in the blade tip region deserves much attention. Naturally, noise emission in the outer blade region can be controlled by keeping the tip speed below a certain value, i.e. by keeping the rotational speed of the wind turbines within limits. However, this measure does not synchronize well with current trends towards building larger wind turbine rotors since a reduction of the tip speed ratio due to a larger rotor would lead to a decrease in energy being captured. Measures other than solely reducing the tip speed ratio have to be applied in the outer blade region. Blade tip shapes optimized for reduced noise emission would allow a wind turbine to operate at optimum tip speed ratio with increased energy capture.

Klug et al. [5] performed noise measurements on full scale outdoor wind turbines with different rotor blade tip shapes and showed that the geometry of the blade tip has a considerable effect on the overall broadband noise level. They reported that modifying the blade tip shape with respect to aerodynamic optimization can lead to a substantial reduction of the noise emission at higher frequencies and reduce the overall noise level by up to 4 dB. The reduction of noise radiation at frequencies between 800 and 7000 Hz can be clearly seen in Fig. 2. These reductions can be very significant when building a wind farm, where aerodynamic noise amplification occurs. Future multi megawatt wind turbines are expected to have bigger rotors and increased tip speed ratios for cost reduction. Thus tip speeds can be expected to increase, throwing new light on the problem of noise emitted from the blade tip.

Fig. 1 WINDMELIII.

The problem of tip noise deserves attention as the physical mechanisms for the generation of tip noise are incompletely understood. Accurate measurements of aerodynamic noise emitted from rotating wind turbine blades are difficult to obtain in wind tunnels and outdoor turbine field tests due to various external factors. Furthermore, experimental measurements do not provide detailed information about the physical phenomena causing aerodynamic noise in the blade tip region. Theoretical interpretations of tip noise did not lead to any definitive conclusions [5]. Thus there is a strong need for accurate prediction of aerodynamic tip noise through large-scale numerical simulations to identify the mechanisms of tip vortex formation and tip noise in order to be able to propose noise reducing design concepts for the outer blade.

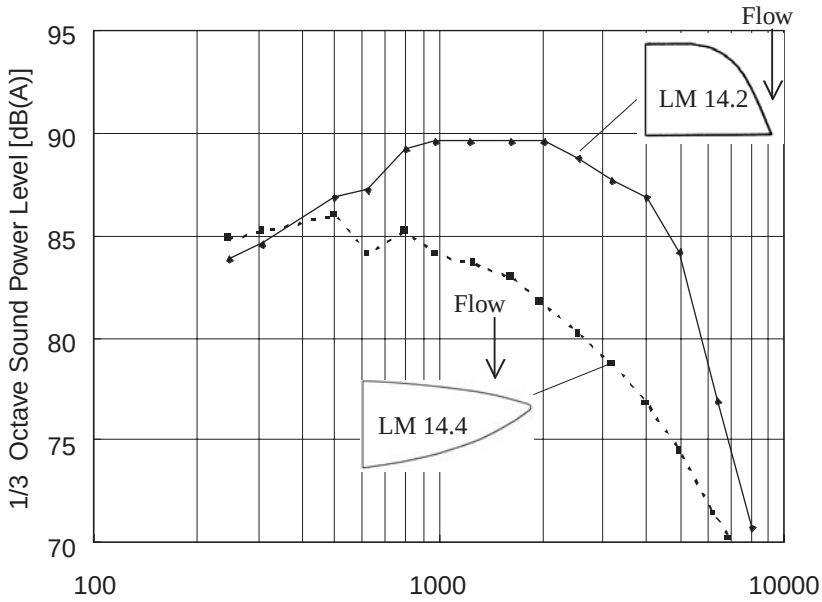

Fig. 2 Blade tip shape influence on wind turbine noise radiation. [5]

1.3 The purpose of this work

There has been no previous work about flow and noise simulation of a full wind turbine blade using CFD. This work constitutes the first attempt. The main purpose of this work is to develop a sophisticated numerical prediction tool for aerodynamic broadband noise emitted by a wind turbine in operation. There is a strong need to devise highly accurate noise simulation techniques which take into account the exact geometry of the wind turbine rotor blade in order to be able to propose noise reducing design concepts and to increase the public acceptance of wind energy.

In this work focus is placed on the tip region of the wind turbine blade. Here, high frequency tip vortex noise constitutes the major noise source. In order to obtain an accurate prediction of the noise sources at the blade tip, the streamwise vortices near the wall must be accurately resolved using a very fine computational grid. This illustrates the requirement for large-scale numerical simulations in order to accurately capture the noise generating turbulent vortical structures. Such large-scale simulations requiring several hundred million grid points have not been performed to date. The present simulation is the first and largest LES direct noise simulation of a full wind turbine blade to date. Simulations using up to 300 million grid points are performed on the Earth Simulator (Yokohama, Japan).

The flow and acoustic field around a rotating blade of the WINDMELIII wind turbine is simulated using compressible Large-Eddy simulation. The time-accurate LES simulation will provide the local aerodynamic noise sources in close proximity to the blades and is able to provide the acoustic field generated at very short distance, a so called direct noise simulation. Far-field noise is predicted by acoustic analogy. Direct noise simulation through the inclusion of compressibility is highly desirable because it provides a more realistic modeling of wave propagation in the vicinity of the surface. Concerning the noise generated in the blade tip region, the wavelength of the noise is much smaller than the blade dimensions. Thus, direct noise simulation can deliver more accurate results for the high frequency domain than previous models that take into account surface pressure fluctuations only. Direct noise simulation also takes into account the inclusion of the feedback effect of the noise on the flow field as well as the quadrupole contribution from vortices and turbulence in near-field. Furthermore, direct noise simulation allows visualization of the acoustic field. Noise sources can be more easily identified and the noise propagation mechanisms better understood.

2. Governing equations and numerical methods

2.1 Fundamentals of compressible flow theory

The first step in the prediction of aerodynamic sound is the investigation of acoustic sources in the flow which generate the sound, especially vortical structures. In this research, the governing equations for the flow are the filtered unsteady three dimensional compressible Navier-Stokes equations in conservative form and generalized coordinates. The flow solver was developed by Matsuo [6]. The numerical method for the solution is based on the implicit finite-difference approach proposed by Beam and Warming [7]. The solution is advanced in time using a

second-order implicit approximate-factorization Beam-Warming scheme with Newtonian sub-iterations and three-point backward differencing for the time derivative. The spatial derivatives are discretized using a third-order finite-difference upwind scheme. The implicit part of the spatial discretization is based on the diagonalization of Pulliam-Chausee [8], the upwind differencing of Steger-Warming [9], the LU factored scheme by Obayashi and Fujii [10]. The effects of the subgrid-scale eddies are modeled using the Smagorinsky model. The Van Driest wall damping function is used to correct the excessive eddy viscosity predicted by the Smagorinsky model near the wall.

So far, wind turbines have often been analyzed using incompressible or pseudo- compressible CFD codes. However, due to the increase in turbine size and higher tip speed ratio, it becomes increasingly important to take compressibility effects into account. The tip speed of future large wind turbines could happen to exceed a Mach number of 0.3, a critical value above which compressibility effects cannot be neglected. Furthermore, inclusion of compressibility is desirable for noise problems. A compressible flow solver can represent acoustic problems more accurately than an incompressible flow solver by accommodating variations in density.

In the region lying in close proximity to the blade the acoustic field is simulated directly using the compressible flow solver. Concerning the noise in the far-field, acoustic analogy methods that do not require a computational grid are used. The simulations are performed in parallel on Earth Simulator, using a domain decomposition approach with pipeline method.

This section constitutes of a brief explanation of the fundamentals of compressible flow theory. A derivation of the stated equations with a detailed discussion can be found in [11]. A fluid is a substance whose molecular structure offers no resistance to external shear forces. Even the smallest force causes deformation of a fluid particle. Density and viscosity are the most important properties of fluids. Two major categories of fluids can be distinguished. Flow with constant density is known as incompressible flow. On the other hand, compressible flow denotes flows that have variable density and temperature. Furthermore, the ratio of the flow speed to the speed of sound in the fluid, known as the Mach number, determines whether exchange between kinetic energy of the motion and internal degrees of freedoms needs to be considered. Incompressible flows are normally associated with flow speeds that are small compared with the speed of sound, i.e. Mach numbers smaller than 0.3. Conversely, compressible flows will imply that the Mach number is greater than 0.3.

2.2 Turbulence modeling

Turbulence modeling remains a key challenge in CFD. Turbulent transport concerns transport from the large eddies to the smallest eddies in the flow. In order to capture this diffusion process with the Navier-Stokes equations, the smallest eddy scales that are known as Kolmogorov scales have to be captured, requiring a grid spacing and time scale that is smaller than Kolmogorov scales. Such an approach is known as Direct Numerical Simulation (DNS). DNS involves resolving all scales of motion in the flow field without any form of modeling. It can be considered the most accurate numerical method as it requires no empiricism. However, DNS requires a very fine grid resolution to resolve all turbulent eddy scales down to the Kolmogorov length scale. As a result, DNS is very costly in terms of computation time. Piomelli and Balaras [12] analyzed the resolution requirements of DNS and suggest that the number of grid points required to fully resolve three dimensional flows is approximately proportional to $Re^{9/4}$. As the Reynolds number increases, this growth relationship results in exponential demands in computing power. Spalart [13] estimates that the number of grid points required to perform a DNS over a complete aircraft at a Reynolds number in the order of 10^7 is approximately 10^{16}. The computational requirements of DNS for flows in engineering applications are extremely difficult to satisfy with current computer resources. It can be said that DNS will remain too expensive for most engineering applications in the near future.

Various turbulence modeling strategies have been developed to reduce computing requirements. These strategies generally use averaged quantities and empirical data to reduce the amount of flow detail that needs to be simulated. A popular turbulence modeling strategy used in numerical simulation is RANS (Reynolds-averaged Navier-Stokes equations). RANS can be used to resolve a turbulent flow with considerably less computational effort than DNS. All of the unsteadiness is averaged out, i.e. all unsteadiness is regarded as part of the turbulence. Following this so called Reynolds averaging operation, details of the instantaneous fluctuations in the flow are lost. On averaging, the non-linearity of the Navier-Stokes equations gives rise to terms that require to be modeled. This term is known as the Reynolds stress tensor, and is associated with correlations between the various velocity components. It arises because the flow fluctuations are not statistically independent and need to be determined by a statistical turbulence model. Since turbulent flows are very complex, it is difficult for a single model to represent all turbulent flows. A popular RANS turbulence model is the k-e model.

Since the main interest of this research is aerodynamic

noise, RANS cannot be used as it cannot adequately supply the pressure fluctuations needed for broadband aerodynamic noise prediction. The loss of unsteady flow detail, incurred by RANS, provides a strong motivation to pursue more accurate turbulence modeling strategies for aerodynamic noise prediction. Although DNS is not feasible at Reynolds numbers occurring in engineering applications such as wind turbines, computing performance has now reached the stage where it possible to perform Large-Eddy Simulation (LES) for various engineering applications.

LES can be considered as an intermediate between DNS and RANS. LES, while yielding more flow detail than RANS and being significantly more accurate than RANS in situations involving flow separation and reattachment, is considerably cheaper than DNS. In an LES approach, it is recognized that the large turbulent structures are generally much more energetic than the small scale ones and their size and strength make them by far the most effective transporters of the conserved properties. The small scales are normally much weaker, and provide little transport of these properties. These large structures are resolved to ensure accuracy, while scales smaller than the size of the computational mesh are modeled. Since these small subgrid scales tend to be more homogeneous and isotropic than the large structures, they can be reasonably represented by a universal model [12]. Moreover, as the subgrid scales only contribute a small fraction of the total turbulent stress, the reliance on modeling should not introduce a large error.

Today, LES can be more readily applied to engineering applications than DNS. LES more directly addresses the physics of turbulence without introducing Reynolds closure approximations. LES is the method used in this research.

LES is based on the concept of filtering. Leonard [14] applied a spatial filter, with a width of grid to separate and remove subgrid scales (SGS) that are smaller than grid size. The filtering separates the resolvable scale, from the subgrid scales. The large or resolved scale field is essentially a local average of the complete field.

As LES does not resolve dissipative subgrid scales, their energy drain on the resolved scales needs to be modeled by the use of a SGS model. The eddy viscosity model proposed by Smagorinsky [15] is one of the most widely used model for SGS closure. It is based on the notion that the effects of the SGS Reynolds stress are increased transport and dissipation. The model assumes the SGS stresses follow a gradient-diffusion process, similar to molecular motion.

The Van Driest wall damping function [16] is used to reduce the value of the eddy viscosity, and hence energy drain, predicted by the Smagorinsky model near the wall. The Van Driest damping function is given in the following expression.

2.3 Direct simulation of aerodynamic noise by Navier-Stokes equations

Acoustic waves are caused by hydrodynamic pressure fluctuations in the flow. The basic equations governing fluid motion and sound propagation are the same. The compressible Navier-Stokes equations contain the equations governing sound propagation and are thus able to simultaneously model the acoustic field in addition to the flow field. Sound waves are a propagating pressure perturbation superimposed on the mean flow field. The perturbations travel at the speed of sound of the fluid medium.

With sufficiently fine grids in the noise generating regions as well as in the far-field, the full non-linear compressible Navier-Stokes equations could be solved for the flow and the acoustic far-field to predict noise generation and propagation, leading directly to the far-field sound. This is called direct noise simulation. Simultaneous numerical simulation of the flow and the acoustic field around a wind turbine blade, i.e. at high Reynolds number and moderate Mach number, is a computationally expensive task due to the large disparity between hydrodynamic flow and the acoustic variables and because the entire far-field domain must be meshed with an adequate resolution with respect to the smallest acoustic wavelength. Since the wave length scale of the sound is much larger than the eddy length scale, the amplitude of the pressure fluctuations associated with the radiated sound is a few orders of magnitude smaller than typical hydrodynamic pressure fluctuations. Diffusion and dispersion errors can easily occur over long propagation distances. Thus the simulation of the acoustic field requires a good numerical wave solution with minimal numerical dispersion and dissipation to prevent the acoustic oscillations from being damped out and to ensure numerical accuracy of the propagation of acoustic waves. A good numerical scheme should preserve both the amplitude and the phase of acoustic disturbances and must support wave propagation with minimized dispersive and dissipative errors over long propagation distances. Tam et al [17] developed robust higher-order finite-difference numerical schemes for wave propagation problems, known as the DRP (Dispersion- Relation-Preserving) scheme. The DRP scheme is optimized for the prediction of wave propagation in its dispersive and dissipative characteristics. When using a third-order upwind finite-difference scheme such as in the present research, a very fine grid is needed to compensate for the dissipation effect in order to realize a high quality direct noise simulation.

Various methods can be applied for the direct simulation of the acoustic field and the unsteady flow field, such as RANS, LES and DNS. In this research, LES is used to determine the noise generating vortical structures. As already mentioned in the introduction, LES is a promising tool for aeroacoustic problems as it can provide the time-accurate unsteady pressure field. LES resolves the noise generating eddies over a wide range of length scales in engineering applications. It is believed that large scales are more efficient than smaller scales for radiating sound. However, Piomelli [18] states that although the contribution of the small scales of motion to the momentum balance is small and can be modeled fairly accurately, the second derivatives of T_{ij} that affect the pressure disturbance will be more significantly affected by the small scales. They illustrate the need to develop subgrid scale acoustic models in order to accurately predict the high frequency noise associated with the unresolved scales. LES can be applied without major adjustments to the subgrid scale model if the bulk of the noise, at least at frequencies of interest, comes from scales that are retained in the simulation and do not have to be modeled. In the present research, the computational grid is made extremely fine in the region of noise generation near the blades to resolve the smallest length scales.

2.4 Acoustic analogy methods

The aerodynamic sound generated from the turbulent wake can be predicted based on acoustic analogy. Lighthill ([19], [20]) derived an inhomogeneous wave equation for the acoustic density fluctuations from the fundamental conservation laws of motion assuming a homogeneous environment at rest. This equation is commonly known as the acoustic analogy or Lighthill's analogy. The far-field sound pressure is given in terms of a volume integral over the domain containing the sound source. Lighhill's analogy cannot be easily applied for arbitrary geometries. It does not take into account the effects of the mean flow, i.e. convection effects, and solid boundaries on the acoustic properties, i.e. refraction effects. Several variations and extensions to Lighthill's Acoustic Analogy exist which allow for mean flow and solid boundary effects. Examples include the formulations by Curle [21] and the Ffowcs-Williams and Hawkings equation [22], the latter being able to take into account the effects of moving solid boundaries on acoustics. All acoustic analogy methods require accurate flow field information from CFD. The computational requirements of acoustic analogy methods are much less than the requirements for LES solutions as the former do not require a computational mesh.

The Ffowcs Williams-Hawkings (FW-H) equation was derived by FW-H in 1969 and has been widely used for the successful prediction of the noise of helicopter rotors, propellers and fans. The FW-H equation is the most general form of the Lighthill acoustic analogy and can be used to predict the noise generated by complex arbitrary motions. This is relevant for the present research as wind turbines rotate. The FW-H equation is based on an analytical formula which relates the far-field pressure to integrals over a closed surface that surrounds all or most of the acoustic sources. In the same way as Lighhill and Curle's equations, the FW-H equation requires the pressure fluctuations from the flow solution as input. Since it is based on the conservation laws of fluid mechanics the FW-H approach can include non-linear flow effects in the surface integration and does not need to completely surround the non-linear flow region. The FW-H equation is an exact rearrangement of the continuity and the momentum equations into the form of an inhomogeneous wave equation with two surface source terms (monopole and dipole) and a volume source term (quadrupole). The computation of the quadrupole contribution requires volume integration of the entire source region and can be difficult to implement. It is common in the FW-H derivation to assume that the surface is coincident with the physical body surface and that it is impenetrable. The assumption that the integration surface coincides with the body surface is not necessary. The FW-H equation has also been applied to permeable surfaces surrounding all physical noise sources.

The FW-H equation on a fictitious permeable surface which does not coincide with the body surface has been investigated by di Francescantonio. Di Francescantonio [23] showed that when the FW-H approach is applied on a surface surrounding the noise generating region, the quadrupole sources enclosed within the surface are accounted for by the surface sources. He demonstrated that for far-field noise prediction the FW-H approach can be used on a fictitious surface that does not correspond with a physical body. However, the "thickness" noise and the "loading" noise as obtained from solving the FW-H equation do not have any physical significance if the surface of integration is chosen to be permeable. When the integration surface is identical with the body surface, these terms provide a physical insight into the source of sound generation. This can help to find design methods for reduced noise emission.

2.5 Boundary conditions for acoustics

The treatment of boundary conditions forms an essential part in aeroacoustic simulations. It is important to set up proper non-reflecting boundary conditions at the outer boundary to prevent acoustic waves from being reflected

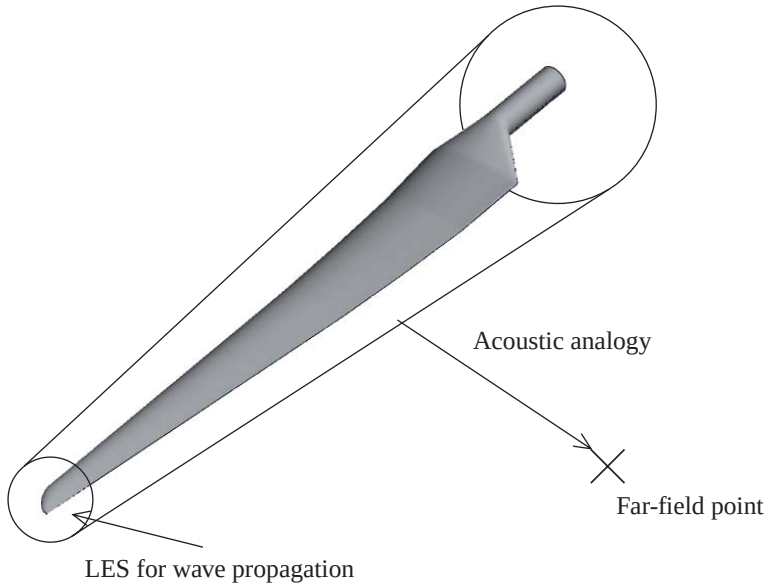

Fig. 3 Method of noise simulation. (Blade type: WINDMELIII)

back into the computational domain. Convective boundary conditions, as implemented in the LES solution, are usually not sufficient to prevent wave reflection at the outer boundaries. Tam et al. [17] proposed non-reflecting boundary conditions which are suitable for acoustic problems.

In this research, non-reflecting conditions are taken care of by grid stretching. A coarse grid acts like a low pass filter. When an outgoing acoustic wave enters the region of grid stretching, it becomes under-resolved in the coarsened grid. Since the present numerical scheme, a third-order upwind scheme, has a tendency to quickly dissipate disturbances in unresolved scales, the numerical solutions are attenuated through numerical dissipation. Care must be taken to avoid abrupt grid stretching in order to prevent grid to grid reflections. This may lead to a very large exit zone with many grid points wasted. Since the computational boundary in the present research is located relatively far away from the region of direct noise simulation, it can be thought that acoustic waves are dissipated long before they reach the outer boundary.

2.6 Noise prediction method – Coupling of LES with acoustic analogy

CFD methods can be coupled with the more efficient integral methods to propagate acoustic signals to the far-field. The noise prediction method employed in this research couples the near-field unsteady compressible LES data with an FW-H formulation for the far-field noise prediction. In the non-linear flow region in close proximity to the blade, that is the region lying 1 to 2 chord lengths away from the blade, flow and acoustic calculations are performed simultaneously in a unique run. This region is called the near-field. The methodology is shown in Fig. 3.

The far-field flow is computed by LES whereas the far-field sound is computed using the permeable surface FW-H method developed by Brentner and Farassat [24]. The time sequence of the acoustic field radiated at the external boundary of the near-field is fed into Eq. (2.149) to obtain sound pressure fluctuations at some point of interest in the far-field.

Direct noise simulation is performed only over a short distance from the blade surface. As diffusion and dispersion errors increase rapidly with large grid size, the grid has to be extremely fine in the near-field to allow for propagation of acoustic waves which are usually four to five orders of magnitude less than the flow fluctuations. The grid spacing and time step in the near-field are determined by the smallest wavelength of interest.

Direct noise simulation can account for refraction and convection effects through the inhomogeneous unsteady flow and reflection and scattering effects on the blade surface. This is essential regarding complex blade geometries. Direct noise simulation also takes into account variations in the speed of acoustic waves. Furthermore, by simulating the propagation of acoustic waves in the near-field directly, the restrictions of the compact body assumption posed by the acoustic analogy methods are relaxed. The acoustic analogy method applied on a surface away from the blade surface is expected to yield more accurate results for the far-field noise in the high frequency domain than would be obtained by solely integrating the blade surface pressure fluctuations. When the smallest wavelength of

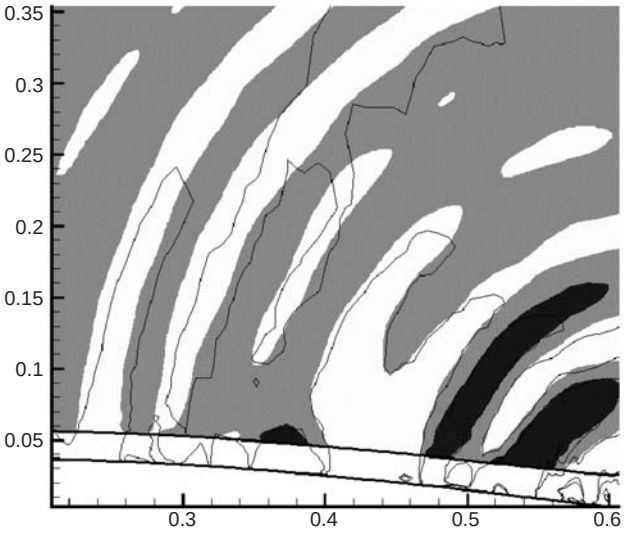

Fig. 4 Isovalue contours of instantaneous pressure fluctuation field computed via LES (black line) overlayed with acoustic analogy data (grey pattern), Manoha et al. [25].

interest is smaller than the body reference length, such as it is the case with trailing edge or tip vortex related noise in high Reynolds number flow, the far-field noise cannot be predicted accurately just by integrating the surface pressure fluctuation such as using Curle's equations. Another advantage of direct noise simulation is that the primary noise sources and vortices responsible for the generation of sound can be identified more precisely through visualization of the acoustic field and physical phenomena of the noise generation process can be studied more extensively. This can contribute to finding new design methods to achieve further noise reduction.

Figure 4. illustrates the discrepancy between the pressure fluctuations obtained by direct noise simulation and the pressure fluctuations obtained by acoustic analogy for flow around a NACA0012 blade section ([25]). LES data contours are plotted using solid black lines, while acoustic analogy data use grey patterns. The waves propagating in the LES domain are slightly slower than the waves propagating in the acoustic analogy domain. This is explained by the fact that the acoustic analogy method assumes uniform flow velocity, while the flow simulated by LES takes into account local velocities that might differ significantly from the uniform mean flow velocity. Acoustic analogy methods do not take into account inhomogeneities of the mean flow outside the integration surface. This is a significant limitation of the acoustic analogy methods. As seen in Fig. 4. discrepancies can be observed even for relatively simple blade section flow at a relatively low Mach number of 0.205. In this case the actual mean flow outside the integration surface assumed in acoustic analogy methods can be considered to be relatively uniform. Regarding more complex flows such as flow around the wind turbine blade tip, discrepancies between direct noise simulation and acoustic analogy methods can be expected to be more evident due to the larger velocity gradients and non-linear flow features in the near blade region.

2.7 Parallelization strategy

Efficient implementation of implicit finite-difference schemes on parallel computers is not straightforward. A pipelined type approach is adopted in this research, according to Aoyama [26]. The main disadvantage of the pipeline method is the idle time and communication latency time of the processors at the beginning of the computations and when the algorithm switches from the forward to the backward computational step. The processors must wait for completion of computations on the previous processors. There is a startup time required for all processors to participate in the computation. The parallel pipelined algorithm applied in this work produces exactly the same solution as its single-processor equivalent.

Parallelization is achieved using the domain decomposition method and MPI. The domain is split in the spanwise direction only. The pipeline method is used for the implicit calculation in the spanwise direction. Parallel efficiency can be kept at around 80 % due to the split in a single direction. The split in the spanwise direction is feasible in the present simulation since the number of grid points is large along the span.

Figure 5. shows the outline of the pipeline method for two dimensional problems. The left hand figure corresponds to the simulation using 1 single processor, while the right-hand side shows the process using 4 separate processors in parallel. Arrows with the same color characterize processes that take place simultaneously. Regarding two dimensional problems, the object transferred between processors is a single element. As for three dimensional problems, the transferred object constitutes a two dimensional array.

3. WINDMELIII flow and acoustics

3.1 Introduction

This chapter describes the simulation of broadband aerodynamic noise and its propagation into the far-field, emitted by a large rotating wind turbine blade of arbitrary shape and with particular emphasis on tip noise. The prediction of aerodynamic tip noise emitted from a wind turbine blade requires the analysis of vortical structures and pressure fluctuations associated with the tip vortex and their interaction with the trailing edge. A large-scale unsteady compressible Large-Eddy Simulation combined with direct noise simulation in the near-field is carried out

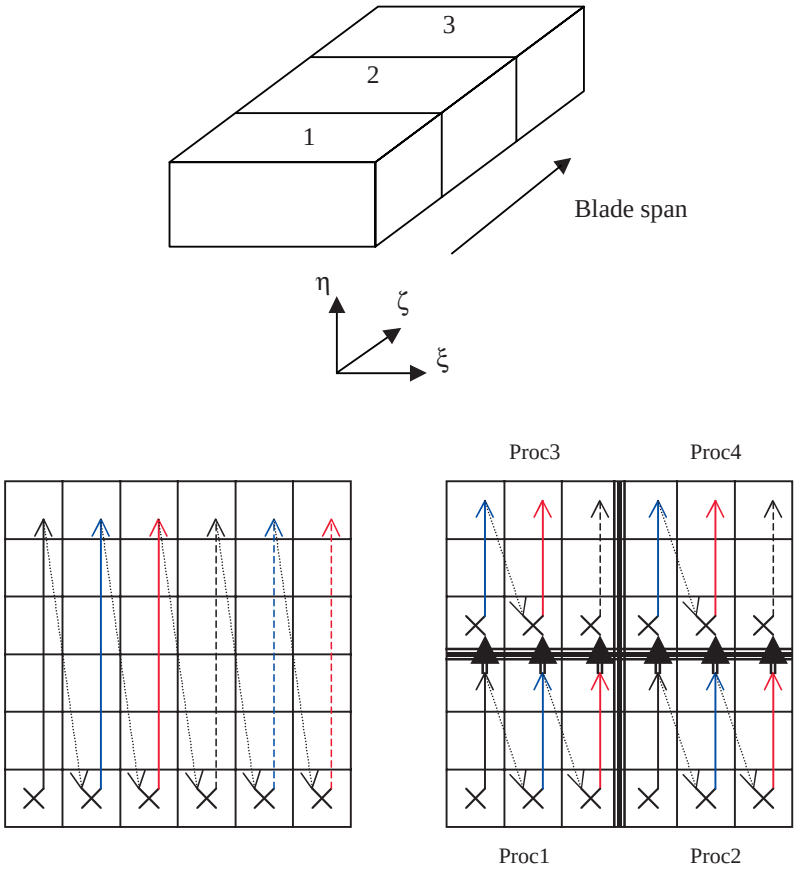

Fig. 5 Pipeline method (2 dimensions) – 4 Processors.

on the Earth Simulator to predict the far-field aerodynamic noise caused by the rotating WINDMELIII wind turbine at the design condition. Concerning the near-field, flow and acoustics are solved with the same code, while the far-field aerodynamic noise is predicted using acoustic analogy methods. The present simulation focuses on the tip vortex noise that is generated in the tip region, i.e. the region with highest velocities. Simulations for the WINDMELIII wind turbine rotor blades are performed for two blade tip geometries, using an extremely fine grid to resolve the smallest eddy scales. The simulation of two different geometries allows investigating the effect of the blade tip shape on the overall aerodynamic noise radiated by the wind turbine. A better understanding of the physical phenomena of tip vortex noise and a comparison of the level of tip noise emitted by different blade tip shapes will contribute towards designing new wind turbine blades and blade tip shapes with reduced noise emission, leading to increased public acceptance of wind energy. In this work, low frequency wind turbine aerodynamic noise is not addressed. It can be thought that this type of noise, mostly caused by blade-tower interaction, is not strongly related to the geometry of the wind turbine blades.

Due to lack of suitable experimental data concerning wind turbine noise, no definite quantitative comparison of the predicted far-field noise spectra with experimental noise measurements has been made at the moment. The accuracy of the computational results is based on the validation cases for basic flows of NACA blades. The results presented in this work provide information about the effect of the blade tip shape on the noise level in a relative sense. Relative changes in the noise level can be predicted accurately by the present large-scale LES. In contrast to predictions of aerodynamic performance such as the power and thrust coefficients, it is often not overly important to obtain exact absolute values for the noise emitted by a wind turbine blade. Rather relative comparisons among different shapes are sought.

3.2 Flow conditions and geometry

The numerical simulation is carried out in accordance with an acoustic measurement experiment of a WINDMELIII test turbine performed by Nii et al. [4]. The two-bladed wind turbine of upwind type has a diameter of 15 m and operates at a wind speed of 8 m/s with a constant speed of 67.9 rpm for the acoustic tests. The rated power output is 16.5 kW. The tip speed ratio is 7.5 and the tip speed is 53.3 m/s, corresponding to a Mach number of

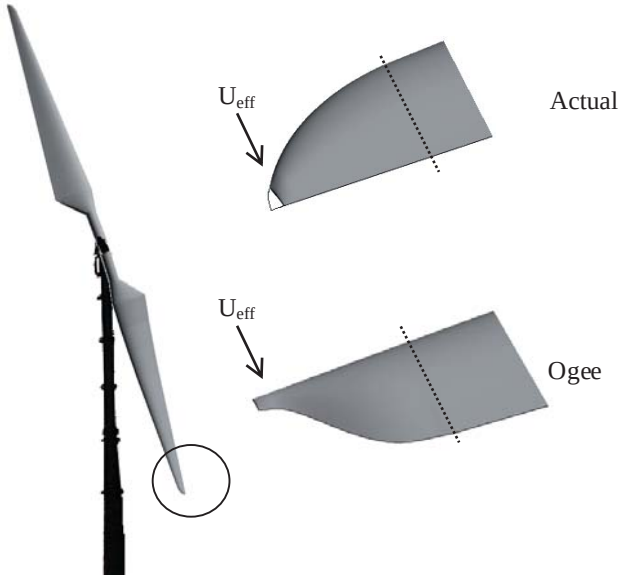

Fig. 6 WINDMELIII – Blade tip shape.

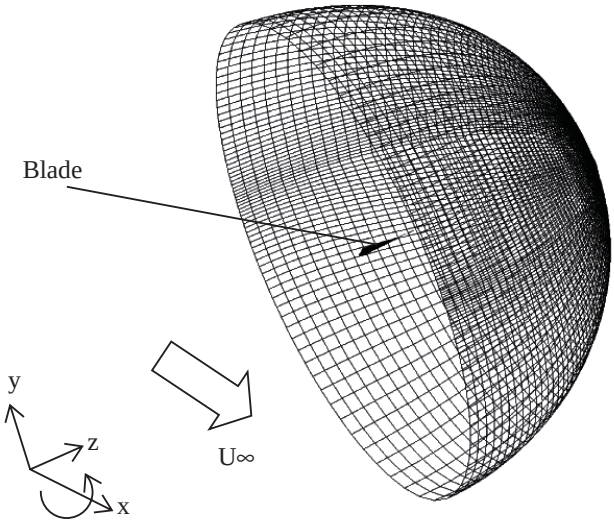

Fig. 7 Computational domain.

0.16. The computation was performed at the design tip speed ratio of 7.5 only.

The actual tip shape of the rotor blades has a curved leading edge and straight trailing edge, as illustrated on the top of Fig. 6. U_{eff} is the effective flow velocity at a particular blade section. In contrast to the real blade, the chord length in the simulation does not reduce to zero at the blade tip due to the use of a single block grid in the present simulation. An ogee type tip shape is also simulated, as shown on the bottom of Fig. 6. The ogee type tip shape has been found in various wind tunnel experiments and outdoor noise measurements on wind turbines to be noise suppressing ([5]). The details of the ogee type tip geometry can be found in Wagner at al. [2]. The term ogee stands for S-arch. The chord length corresponding to the dotted line in Fig. 6. will be referred to as the reference chord length which equals 0.23 m. This corresponds to radial position r/R = 0.95 and is the spanwise location beyond which the blade shape differs between actual and ogee type tip shape. At the design condition of WINDMELIII the Reynolds number based on the reference chord length and the effective flow velocity at the reference chord length is 1.0×10^6.

3.3 Computational grid

The computational domain for the wind turbine blade is illustrated in Fig. 7. A single block grid is used. Since the wind turbine has 2 blades, the domain is chosen to consist of half a sphere. Only one of the blades is explicitly modeled in the simulation. The remaining blade is accounted for using periodic boundary conditions, exploiting the 180 degrees symmetry of the two-bladed rotor. Uniform flow, $U\infty$, corresponding to the wind speed is prescribed in the -x-direction. The blade rotates about the x-axis. The outer boundary of the computational domain is located 5 rotor radii away from the center of rotation. The detailed geometry of the hub and the wind turbine tower are not taken into account in the simulation. The wind turbine blade flow in this work is treated with the same numerical algorithm as in the previous chapter. The simulation is performed in a rotating frame of reference. Eddy scales as fine as the ones simulated in the preliminary simulation for NACA blades will be resolved, at least in the blade tip region.

Concerning the boundary conditions, no-slip conditions are applied at the wall, and pressure and density are extrapolated. Convective boundary conditions are implemented at the outlet. Outer boundaries are made coarse enough to allow for non-reflecting acoustic boundary conditions, as described in section of 2.5. In this work, the computational domain extends extremely far away from the blade, i.e. 200 times the chord length or 5 times the rotor radius, while direct noise simulation is performed only in the near-field, i.e. 1-2 chord lengths away from the rotor blade. Due to the large rate of stretching and the extreme distance between the blade and the outer boundaries, high frequency fluctuations and even low frequency fluctuations can be considered to be filtered out before reaching the outer boundary. It must also be noted that numerical dissipation with the third-order upwind scheme is high in the outer regions due to the coarse grid. Acoustic waves will be dissipated.

Inflow conditions are prescribed without fluctuations. This means that the flow is uniform at the inlet, with tur-

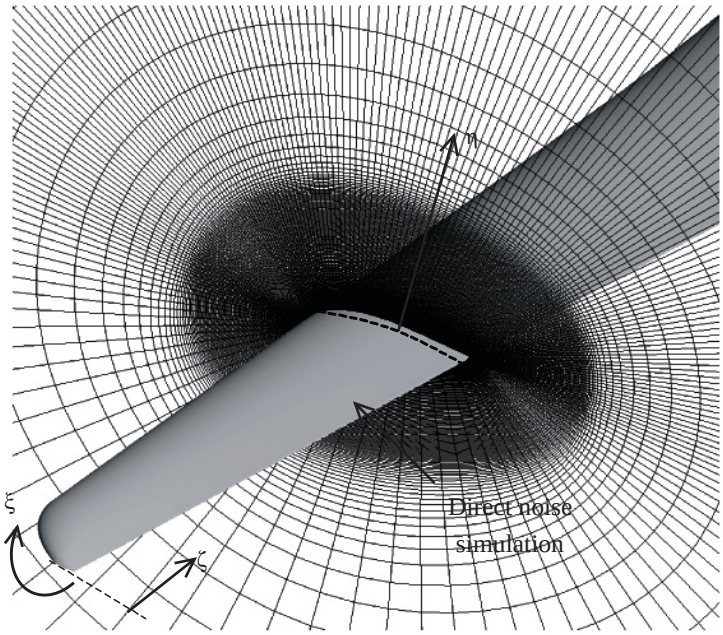

Fig. 8 Grid of Airfoil section – ζ plane (*Grid1*).

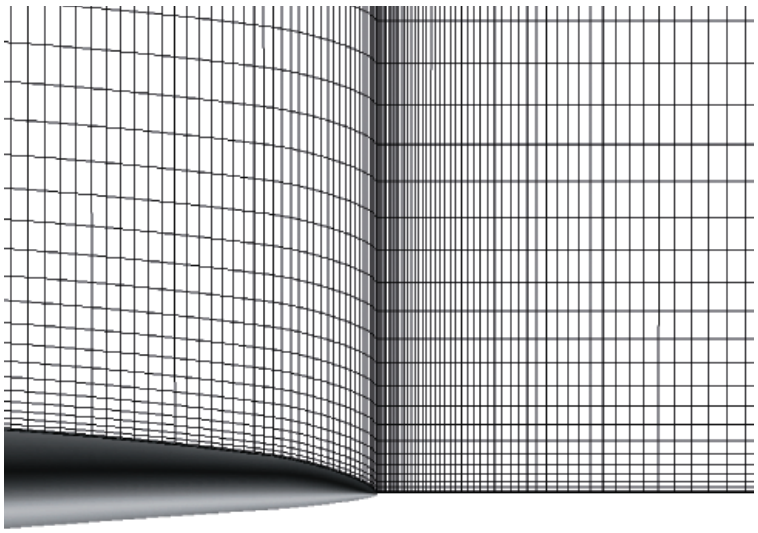

Fig. 9 Grid of Airfoil section – ξ plane (*Grid1*).

bulent fluctuations being neglected. In reality, the inflow contains a considerable amount of turbulence which should ideally be taken into account in the simulation, especially since the experimental measurements on the WINDMELIII are performed in conditions with strong wind speed fluctuations. The broadband noise is said to depend strongly on the level of inflow turbulence. Alternative treatments of inflow boundary conditions include prescribing turbulent inflow conditions with random fluctuations. This can be accomplished by assuring that the inflow has the proper kinetic energy. However, it is common that random fluctuations dissipate quickly without sustaining or initiating turbulence. The random fluctuations could however act as initial disturbance, which could be important for natural transition from laminar flow to turbulent flow.

Druault et al. [27] proposed a method for generating realistic inflow conditions based on two-point statistics

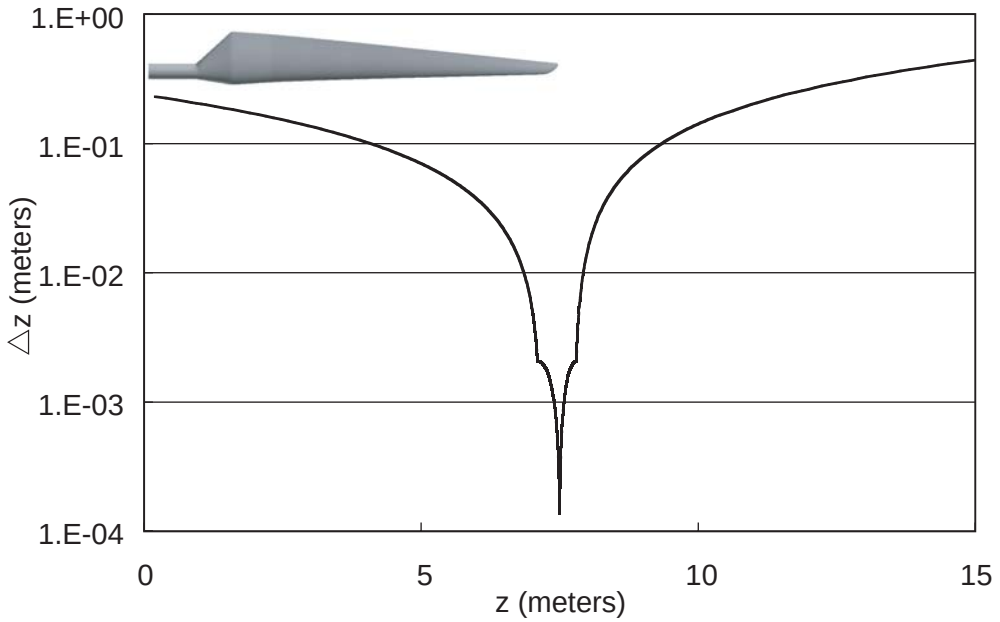

Fig. 10 Spanwise grid spacing along WINDMELIII blade (in meters).

and stochastic estimation. The large-scale coherence of the flow is reproduced in space and time. The method is based on linear stochastic estimation. DNS results are used to generate realistic inflow conditions, retaining only a minimum size of relevant information.

Figure 8. shows the computational grid of the wind turbine blade section at radial position $r/R = 0.88$. The grid is called *Grid1*. The computational grid is of O-grid topology consisting of 765 grid points along the airfoil surface and 385 grid points perpendicular to the airfoil surface. The suction side consists of 565 grid points and the pressure side has 201 grid points. No wall model is used. 1113 grid points are taken along the span direction. The total number of grid points is 320 million. The grid spacings in the near blade region are set according to the observations made in the validation part of the preliminary approach in order to perform a direct noise simulation. Since the main interest of this research is tip noise, the computational grid is made extremely fine in the blade tip region. Figure 9. shows the grid at the blade tip. Here, LES requirements for the grid spacing in terms of wall units Δx^+, Δy^+ and Δz^+ are fully satisfied. Δy^+ is set to take a value of approximately 1.0 along the entire blade surface. No wall model is used. At the blade tip, the non-dimensional spanwise grid spacing Δz^+ is 15.0. Δz^+ increases faster in the free zone than on the side of the wind turbine blade due to the absence of the solid wall in the free zone. The spanwise grid spacing along the blade is shown in Fig. 10. The non-dimensional streamwise grid spacing Δx^+ equals approximately 50.0 is the region where transition is to be expected, that is slightly downstream of leading edge. Towards the blade root and in the outer boundary region, the grid spacing is too large to satisfy LES requirements. However, the inner blade region does not contribute much to the overall aerodynamic performance. It can be thought that the effect on the tip vortex noise is small.

In order to satisfy LES grid spacing conditions along the entire span length, the number of grid points would have to be increased considerably. It is estimated that up to 15 billion grid points, with 100,000 grid points along the span, are required to satisfy Δz^+ along the entire blade. Although a simulation with 15 billion grid points could be realized on the Earth Simulator, it is not practical at present.

The largest frequency of interest in the present simulation is 10 kHz. The direct simulation of the acoustic field is performed in the domain lying approximately two chord lengths away from the blade surface. This domain will be referred to as the near-field. In the immediate proximity of the blade, i.e. in the region lying within 1.5 chord lengths away from the blade surface, the resolution per wavelength corresponding to 10 kHz is approximately 25 points per wavelength. This resolution decreases to 20 at a point lying 2 chord lengths away from the blade. Comparison with analytical results for the convection of a small pressure pulse in a uniform flow has shown that in order to achieve an accurate solution with the third-order finite difference scheme approximately 25 to 30 points per wavelength are required. Thus the highest frequency resolvable by the simulation in the region lying 2 chord lengths away from the blade surface would be slightly lower than 10 kHz.

The non-dimensional time step is 4.0×10^{-5} c/U_{eff}. The physical time step is approximately 1.4×10^{-7} seconds, meaning a sampling frequency of 7 MHz. This is more than sufficient to capture the acoustic phenomena associated with the tip vortex. The simulation of the blade with 300 million grid points took 300 CPU hours for 250,000 time steps on the Earth Simulator using 112 processors in parallel. During this period of 50 ms the blade rotates 20.4 degrees and the blade tip moves 2.6 m. The simulation covers 10 non-dimensional time units.

It is essential to discuss the implications of the short rotation time. At present, longer runs are not possible due to a limit in computational time. The present simulation can be considered the first step of large-scale wind turbine flow and noise simulation. The tip vortex will be in a very transient state at this time. It would take many complete rotations of the rotor for a fully developed wake and tip vortex to be established. General observations from rotor computations show that for the tip speed ratio in question 2 to 3 rotor revolutions are required for the flow to build up and to take into account the full flow field and the induction from the vortices in the wake. The time span simulated in this work is sufficiently long to cover the process of tip vortex formation and interaction of tip vortex with the blade trailing edge. The lower boundary of the dominant frequencies of the tip vortex is approximately 3,000 Hz, corresponding to a time span of 0.33 ms, which is much smaller than the simulation period of 50 ms. It can be said that the tip vortex noise generation mechanism and associated acoustics are properly captured in the present simulation. Longer runs including several full rotations would be necessary to carry out for predicting low frequency aerodynamic noise such as blade-tower interaction.

Concerning the aerodynamic performance of the wind turbine blade, longer simulation times are necessary, especially to take into account the induction from the vortices in the wake. Iida et al. [28] performed a RANS simulation of a wind turbine blade using the same numerical temporal and spatial schemes as the present LES solver. They simulated 5 to 6 complete rotations of the rotor, and obtained very good agreement with experimental measurements regarding aerodynamic performance of the wind turbine blade such as overall power and thrust coefficient. However, RANS cannot provide accurate turbulent frequency spectra which in turn are required for high frequency aerodynamic noise. The present LES simulation, although simulating only a fraction of a full rotation, allows relative comparison between different tip shapes in terms of acoustic emission. It can give us new insights into the physical phenomena of tip vortex noise and can predict relative changes in the overall noise level for different tip shapes, a feature which is essential for design purposes.

The present work should be considered a first step towards full LES of a wind turbine blade with the ultimate aim to design wind turbine blade tips with reduced noise emission. LES simulations covering several rotations will become possible in the future with increasing computational resources.

3.4 Flow field in the blade tip region

The flow in the blade tip region of the actual and the ogee type tip shape is investigated in more detail. *Grid1* is being used in the simulation. For clarification purposes, several cross sections are being defined in Fig. 11. *S1* lies parallel to the reference chord and passes through the trailing edge of the blade section corresponding to the reference chord length. Face *S2* is perpendicular to the reference chord length and passes through the leading edge of the blade section corresponding to the reference chord length. *S3* and *S4* are the blade cross sections located at radial positions r/R = 0.88 and r/R = 0.98, respectively. *S4* is located in the region where the blade shape differs between actual and ogee type tip.

The vorticity isosurfaces ωx in the tip region are shown in Fig. 12. for both tip shapes. Vortical structures in the vicinity of a body cause intense noise. Very complex three dimensional vortical flow structures associated with the tip vortex can be identified. For both tip shapes these vortical structures prevail in the immediate vicinity of the trailing edge, suggesting the importance of the tip vortex-trailing edge interaction as a noise contribution. Concerning the actual tip shape, a major part of the vortical structures can be identified at the immediate tip and in the tip vortex, in close proximity to the blades surface. Vortices that exist near the blade surface have greater contribution to the sound generation than those that exist far from the blade surface. The contribution of a vortex to the sound generation decays in inverse proportion to the third power of the distance between the body surface and that particular vortex. As for the ogee type tip shape, the tip vortex structure is smoother than for the actual tip shape. Reduced tip vortex shedding and reduced interaction with the trailing edge suggests reduction of noise. There exists, however, some degree of interaction between the vortical structures and the trailing edge further inboard. For the ogee tip the trailing edge curvature leads to the formation of further but weaker circulation vortices due to local cross flows along the trailing edge. Due to the thin extension a strong leading edge wake is expected to build up and possibly being able to disturb the generation of the tip vortex.

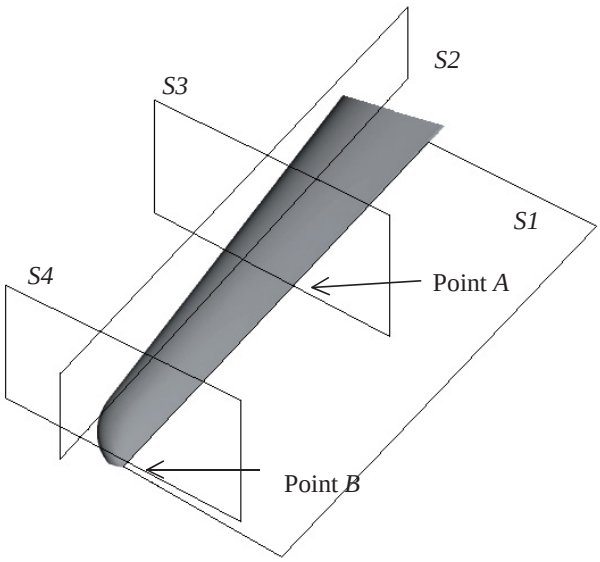

Fig. 11 Definition of cross sections.

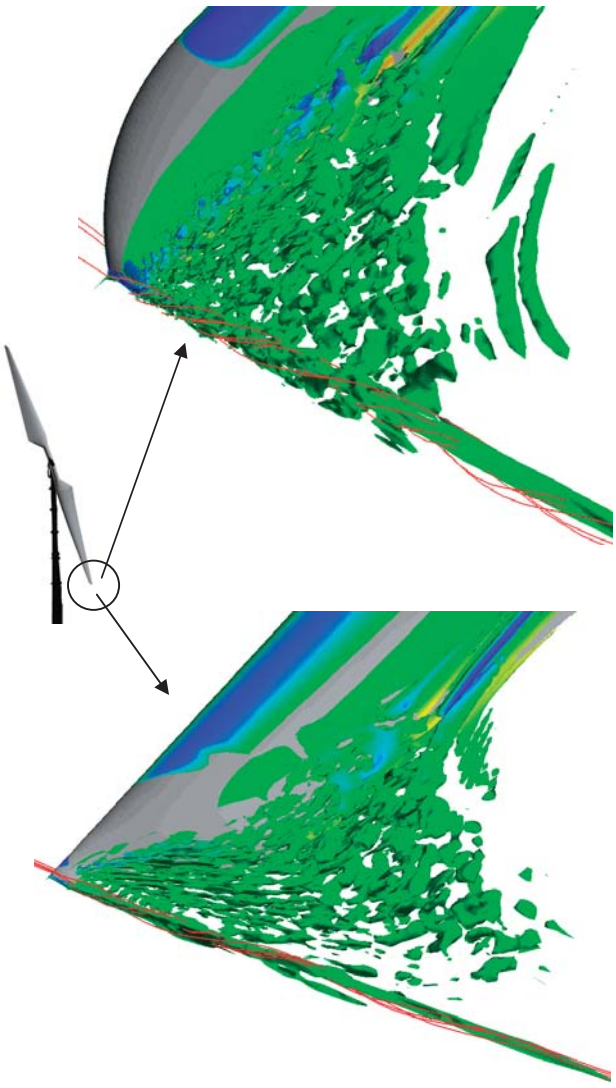

Fig. 12 Vorticity ω_x Isosurfaces (Top: Actual, Bottom: Ogee).

3.5 Pressure fluctuations at blade tip

To evaluate the effect of the difference in the structure of the vortices in the blade tip region on the acoustic near- and far-field, the pressure fluctuations in the near blade region are analyzed and compared between actual and ogee type tip shape. As shown in Fig. 11, the pressure fluctuations are taken at points *A* and *B*. Point *A* and *B* lie slightly downstream of the turbine blade trailing edge, on faces *S3* and *S4*, respectively. *S3* is the region where the blade shape is the same for the actual and ogee type blades. *S4* lies in the region where the blade shape differs. The distance between the trailing edge and point *B* is the same for both the actual and the ogee type tip shape. The flow travels the same distance in both cases. Figures 13 and 14 illustrate the pressure fluctuations taken at points *A* and *B* between 0.02 s and 0.028 s. At point *A* the amplitude and frequencies show very similar values for both tip shapes. However, at point *B*, where the blade shape differs, it can be seen that the amplitude of the pressure fluctuations has decreased for the ogee type tip shape as compared to the actual tip shape. Furthermore, high frequency fluctuations can be observed for the actual tip shape. These high frequency contributions in the blade tip region of the actual tip can be thought of affecting the noise level and frequency in the far-field. Concerning the ogee type tip shape, these high frequency fluctuations do not appear. The ogee type tip shape shows a lower degree of turbulence and weaker noise source in the tip region. It is difficult to measure pressure fluctuations around rotating blades in a wind tunnel. No experimental data of pressure fluctuations is currently available for comparison. However it has been confirmed in the preliminary research that the present numerical method is robust and provides quantitatively accurate results for pressure fluctuations and spectra in the high frequency domain when very fine grids are used.

3.6 Acoustic field

Examination of the surface pressure fluctuations alone does not always provide useful information for aerodynamic sound reduction, especially when studying the sound generated from an object having a complex shape. Powell's sound source term helps to identify vortex generated sound sources.

Powell [29] investigated which characteristics of the turbulent flow or eddy motion are responsible for sound generation and found that the formation and motion of vortices or vorticity is the fundamental noise-producing mechanism. For a relatively high Reynolds number flow with no heat release, the entropy and viscous-stress terms in Lighthill's acoustic tensor can be neglected and the Reynolds-stress term becomes the dominant contributor

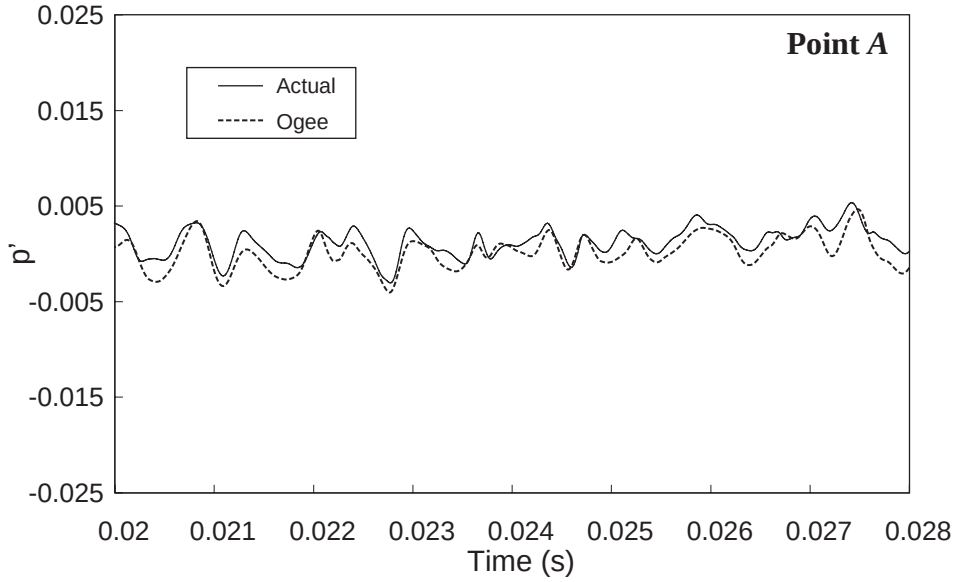

Fig. 13 Pressure fluctuations *p'* at point *A*.

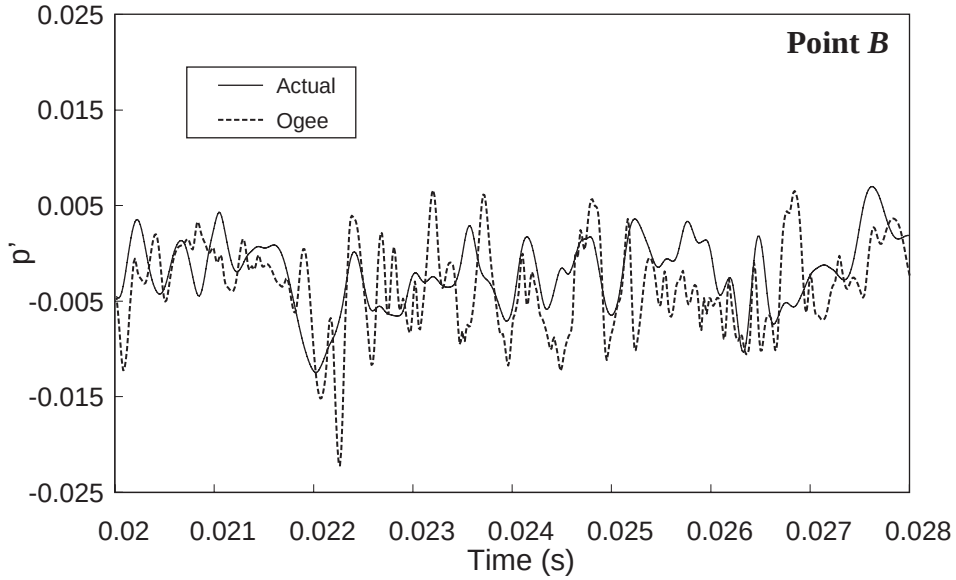

Fig. 14 Pressure fluctuations *p'* at point *B*.

to the sound generation.

$$\left(\frac{\partial^2}{\partial t^2} - a^2 \nabla^2\right)\rho = \nabla \cdot (\rho \boldsymbol{\omega} \times \mathbf{u}) \qquad (1)$$

Equation (1) shows the contributions from the vortical motions in the flow to the sound generation where a, $\boldsymbol{\omega}$, and $\mathbf{u}$ show sound velocity, density, vortex and velocity respectively. Sound sources in the near wake can now be identified based on the instantaneous values for the right-hand side of Eq. (1).

Figure 15 shows the distribution of instantaneous values of Powell's sound source term Div·(u×ω) on face *S1*. The sound source intensity maps can be used to detect dominant noise origins. Powell's sound source shows the most relevant sound sources of vortex generated aerodynamic sound for low-speed flow.

Through the analysis of Fig. 15 the vortical structures that contribute most to the generation of the far-field sound can be identified. The primary source of aerodynamic sound is unsteady motion of vortices in regions close to the blade. Regarding the actual tip shape, a concentration of high values of Powell's sound source can be identified immediately downstream of the trailing edge at the tip. These sound sources near the blade surface can be

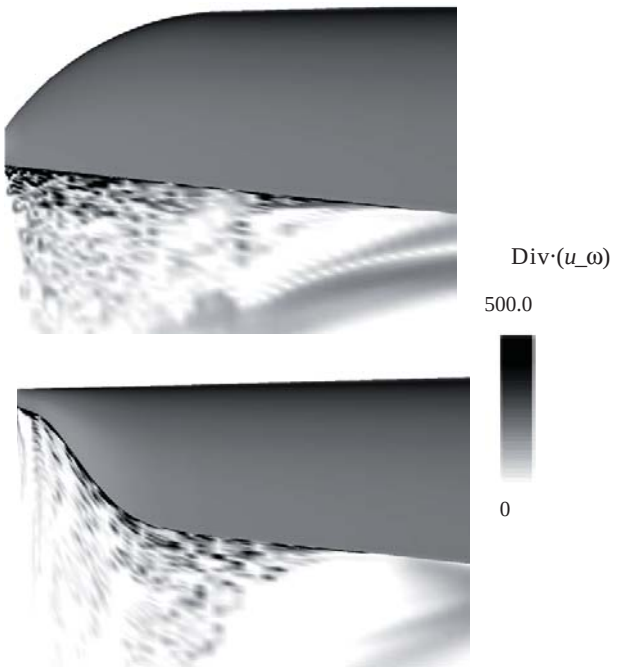

Fig. 15 Div· (*u_ω*) on *S1*.

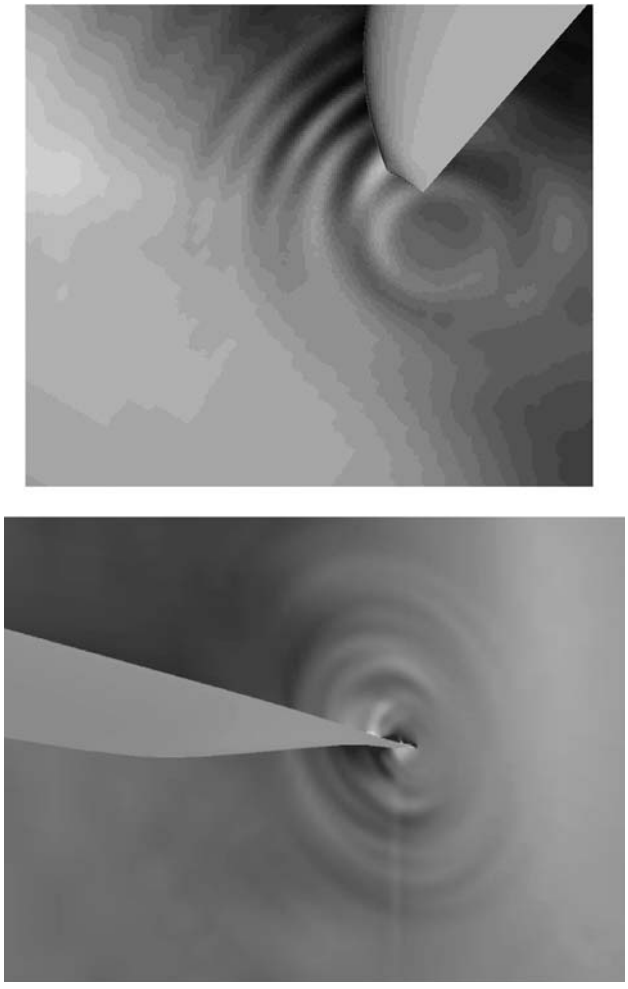

Fig. 16 Instantaneous pressure perturbation field on S2. (Top: Actual, Bottom: ogee)

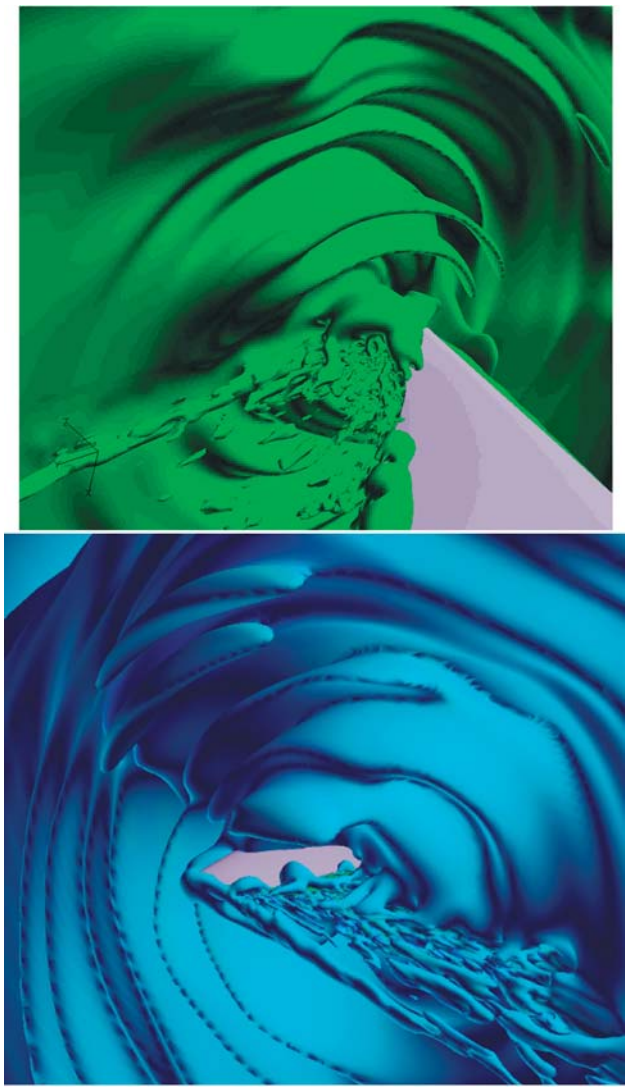

Fig. 17 Instantaneous pressure perturbation isosurfaces. (Ogee type tip shape)

expected to contribute strongly to the far-field noise. Vortices generated by the actual blade in the tip region are identified as being primarily responsible for the generation of sound by this flow. In general complex structures are less prevalent and more equally distributed along the blade trailing edge for the ogee type tip shape, without being concentrated in the blade tip region. The values of Powell's sound source are lower on average for the ogee type tip shape than for the actual tip shape.

Figure 16 shows the instantaneous pressure perturbation field of the wind turbine blade with ogee type tip shape obtained by direct LES on face *S2*. Pressure fluctuations on the blade surface constitute an acoustic source and propagate into the far-field. They are the main cause for aerodynamic noise. The compressible LES flow solver is able to simultaneously simulate the propagation of the acoustic waves caused by the surface pressure fluctuations away from the blade in addition to the unsteady

flow field.

Figure 17 shows the pressure perturbation isosurfaces in three dimensions for the ogee type tip shape. It can be clearly seen that the noise source lies in the tip region, with acoustic waves propagating away from the tip. The pressure perturbations contain contributions mainly from the fluctuations associated with the tip vortex and its interaction with the trailing edge of the wind turbine blade. The upper figure corresponds to isosurfaces of positive pressure fluctuations whereas the lower figure corresponds to isosurfaces of negative pressure fluctuations. The acoustic field radiates approximately two reference chord lengths away from the blade, as expected from the current grid characteristics.

Concerning Figs. 16 and 17, the number of grid points captured by a wave length corresponding to a frequency of 7 kHz is sufficiently large to allow for accurate propagation of acoustic waves in the near-field.

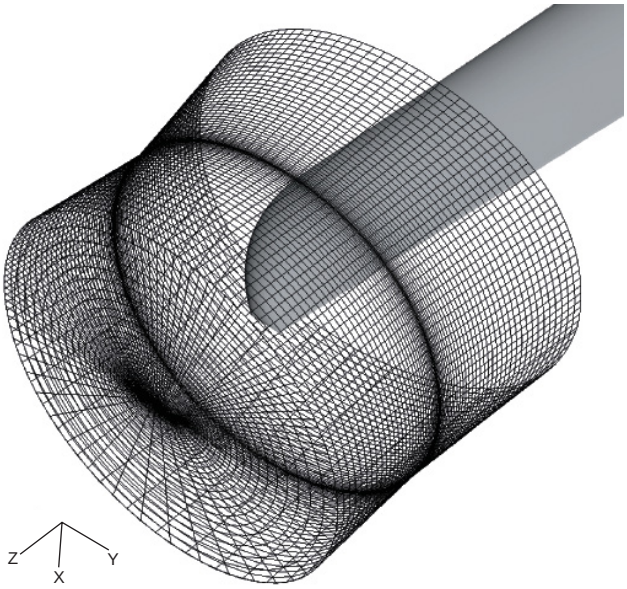

Fig. 18 Integration surface for FW-H.

3.7 Far-field noise prediction

The effect of the blade tip shape on the overall far-field noise level is investigated. Velocity components, density and pressure obtained from LES are stored at prescribed time steps on a fictitious permeable surface lying one reference chord length away from the blade and encircling the blade. The noise perceived in the far-field is computed using acoustic analogy methods by integration of physical quantities on the surface shown in Fig. 18.

The acoustic perturbations evaluated by the LES simulation are integrated using the FW-H equation by Brentner. This integration yields the acoustic pressure level in the far-field. The spectra were obtained by a FFT analysis using a rectangular window. The sample of 7 ms, which corresponds to approximately 10 non-dimensional time units, was divided into 500 records, meaning a frequency resolution of 70 kHz. In terms of grid resolution, 10 kHz, the smallest wavelength of interest, corresponds to $1/7^{th}$ in terms of tip chord length. One wavelength corresponding to 10 kHz is covered by 25 grid points, requiring about 260 grid points in the direction perpendicular to the blade surface in the near-field.

The integration surface has a shape of a cylinder with a tip-end cap. Time-accurate flow data on the permeable FW-H surface is provided by LES in the near-field. In this research, the integration surface used for the FW-H equation is actually used in the LES simulation as well, so no additional interpolation is required. Since a rotating frame of reference is used, the values are converted to stationary values before being fed into the FW-H equation. A numerical integration of Eq. (2.149) is performed by approximating the integral over each grid point. The simulated changes in sound pressure level for the actual and the ogee type tip shapes are shown in Fig. 19 for a far-field observer point located 20 m upstream of the wind turbine.

At 20 m, the effect of the blade tip shape on the aerodynamic noise level in the high frequency domain is obvious. According to the simulation results, the ogee type tip shape shows a decrease in acoustic pressure level for frequencies above 3 kHz. The ogee type tip shape clearly has a noise reducing effect. A reduction of approximately 2 dB is attained for the overall sound pressure level (OASPL). The reduction above frequencies of 3 kHz is approximately 5 dB. The reduced acoustic emission of the ogee tip is likely to be related to the decreased interaction between the tip vortex and the trailing edge. According to the noise measurement experiment [4], a point source is located at the tip of the blade for frequencies from 3.1 kHz to 6.3 kHz, suggesting a small but intense lateral vortex shedding from the tip. Peaks can be observed in this frequency range in Fig. 19, suggesting some agreement between the simulation and the experimental measurements. The removal of small high frequency pressure fluctuations for the ogee type tip shape explained in Section 4.5 can be thought of being the reason for reduced noise radiation.

The simulation results for the observer position located 20 m away from the wind turbine show a similar trend with the measurements obtained by Klug et al. [5] for the noise emission of a blade tip with a curved trailing edge similar to the ogee type tip shape. In Fig. 20, frequencies are non-dimensionalized based on the effective velocity at the tip and the blade tip chord length. The simulation results and the field test measurements show a reduction

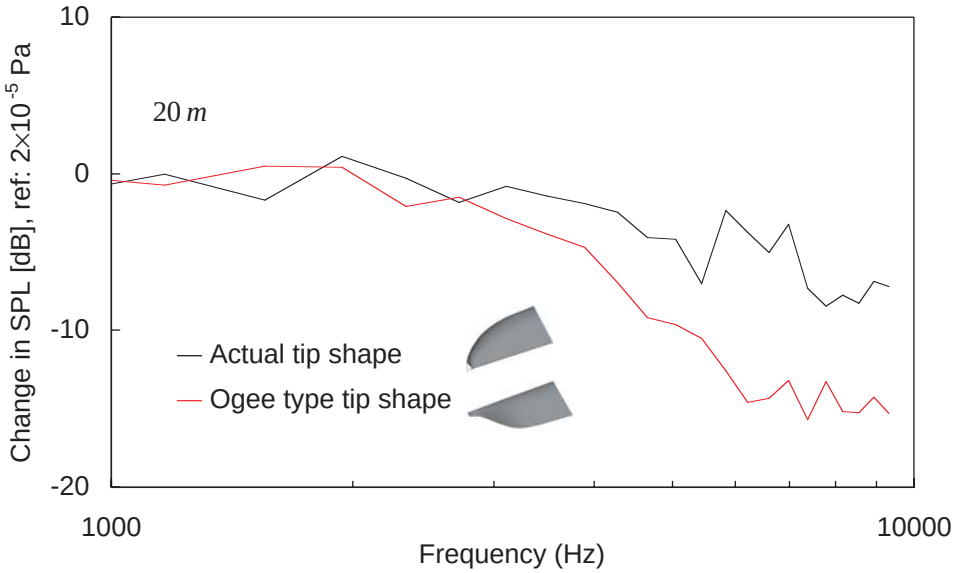

Fig. 19 Sound pressure level – Simulation results – Fictitious FW-H surface.

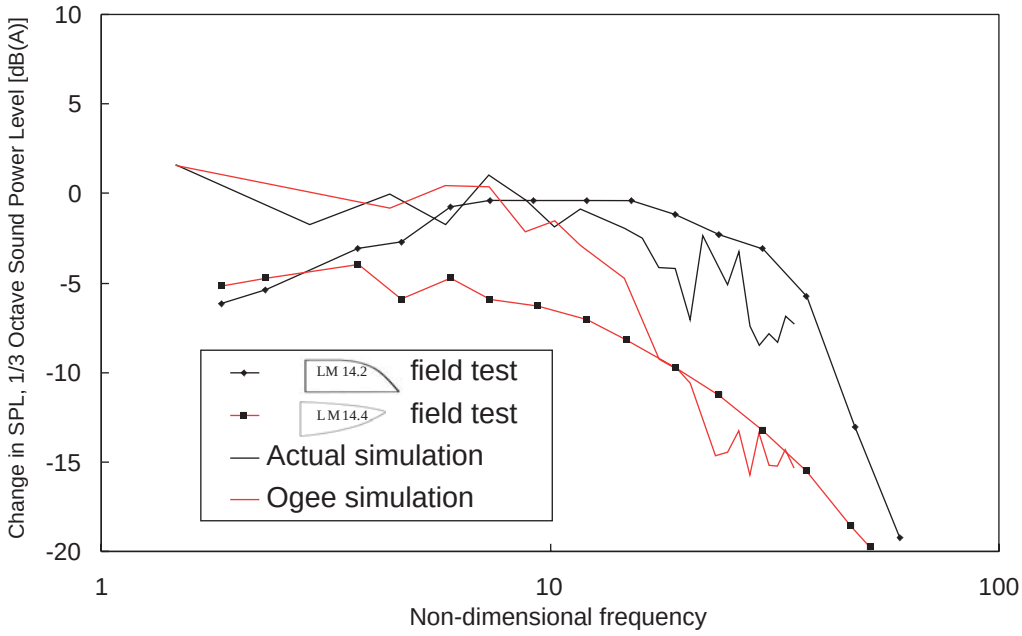

Fig. 20 Tip shape influence on wind turbine noise [5].

of sound pressure level for the ogee type tip shape in the same frequency domain.

Quantitative comparisons between the experimental test turbine measurements by Nii et al. [4] and the computed far-field noise levels are not performed at the moment since the test turbine also emits gear and generator noises from the gearbox and the blade-tower interaction noise. Even though the ultimate aim of this research is without doubt the prediction of the absolute values of the noise level, the grid employed in the present work is not fine enough to satisfy the requirements of Large-Eddy Simulation along the entire span of the wind turbine rotor blade. The grid is too coarse to capture flow and acoustic effects of the inboard section of the blade and in the hub region. Furthermore, the tower is not included in the numerical simulation. However, the test turbine measurements include all types of noise, including mechanical and blade-tower interaction noise. Thus simulation results are not expected to directly agree well with experimental measurements of the noise.

Nii et al. [30] experimentally studied the generation mechanism of noise originating in the tip area of the

WINDMELIII wind turbine. They used a microphone array system to evaluate the acoustic performance of the 15 m diameter experimental wind turbine rotor blade. Results revealed that the blade emits strong high frequency broadband noise from the tip and mid frequency noise from the trailing edge of the blade. They suggest that the noise generation mechanism of high frequency noise is due to the streamwise vortices shed directly from the extreme tip.

The noise at high frequencies does not propagate as far as low frequency noise. As seen from the simulation results, the noise reduction caused by the slight change of the wind turbine blade tip geometry is 2 dB overall. The results obtained by the present large-scale numerical simulation suggest that the high frequency noise emitted in the outer region of the wind turbine blade is indeed relevant as the human ear is most sensitive to frequencies between 1 and 5 kHz. This frequency range can be simulated accurately with the present LES solver.

As mentioned in the introduction, there is a trend towards building larger wind turbines and increasing the tip speed ratio in the future due to cost reasons, possibly using more slender and fewer blades. The levels of high frequency noise caused in the blade tip region can be expected to increase since the high frequency broadband noise emission increases with the fifth or sixth power of the effective flow velocity,. Thus the high frequency noise for which the ogee type tip shape has shown a noise reduction will be a serious concern and cannot be neglected in residential areas in the far-field. Noise reduction in the high frequency domain will be a more relevant issue for future wind turbines. For present wind turbines, the sound in the high frequency domain is not too disturbing in residential areas. A noise level of approximately 40 dB is perceived 200 m away from the wind turbine. It cannot be distinguished from ambient noise since high frequency noise dissipates over short distances. The problem of tip vortex noise clearly deserves attention for future wind turbine applications, and accurate prediction methods for the higher frequency noise are desirable.

3.8 Merits of direct noise simulation

As shown in the previous section, direct noise simulation, even if just carried out in the region in close proximity to the blade, allows the accurate simulation of the most intense quadrupole sources while neglecting the computationally expensive quadrupole volume integration. This is a distinctive advantage of the direct noise simulation in the near-field, as compared to integration of blade surface pressure fluctuations. This also assures that the vorticity contribution and the non-linear effects of flow and sound velocity in the near-field to the overall sound is accurately taken into account.

Monopole and dipole sources are important for a wide range of Mach numbers. Quadrupole sound sources usually become important at relatively high Mach numbers, but they can also appear at lower Mach numbers. The importance of the quadrupole contribution for wind turbines with Mach numbers at the tip ranging from 0.1 to 0.3 was already discussed in the section of 2.8. Quadrupole sources are essential in flow regions with strong flow speed variations such as in the near blade region, in the blade tip vortex and in the turbulent boundary layer. Quadrupole sources are associated with nonlinearities in the flow field caused by both local sound speed variation and finite fluid velocity near the blade surface in the turbulent boundary layer. Although the flow around wind turbine blades is in the low Mach number range, quadrupole sound is generated [2], especially aft of the leading edge on the suction side, due to flow acceleration. The turbulence in the boundary layer radiates quadrupole sound that is scattered at the trailing edge, leading to intense noise radiation at the trailing edge of the blade. The flow speed variations in the tip vortex lead to further quadrupole noise radiation at the tip of the blade.

Concerning non-deterministic noise for subsonic turbulent flows, such as high frequency noise from wind turbines, the primary sound sources are the fluctuating Reynolds stresses. This corresponds to quadrupole sound. In the presence of rigid surfaces, the sound is reflected, scattered, or diffracted at the surface. This leads to additional monopole and dipole sound [2]. Sound with quadrupole character occurs in all turbulent flows. The physical mechanism can be described by a system of normal and shear stresses as well as fluctuating Reynolds stresses. The strength of quadrupole sound sources is determined by the Lighthill tensor.

In section of 2.5 the merits of direct noise simulation over acoustic analogy were shown. Discrepancies between the pressure fluctuations obtained by direct noise simulation and the pressure fluctuations obtained by acoustic analogy for flow around a NACA0012 blade section were observed even for relatively simple blade section flow at a relatively low Mach number of 0.205. In this case the actual mean flow outside the integration surface can be considered to be relatively uniform. It was seen that the acoustic waves propagate at different speeds in the LES domain and in the acoustic analogy domain. This is because the acoustic analogy method assumes uniform flow velocity, while the flow simulated by LES takes into account local velocities that can differ significantly from the uniform mean flow velocity. Furthermore, acoustic analogy methods do not take into

account inhomogeneities of the mean flow outside the integration surface. This is a significant limitation of the acoustic analogy methods.

By performing a direct noise simulation, the above-described non-linear effects in the near blade region are taken into account considerably more accurately than in acoustic analogy methods. Furthermore, the quadrupole contribution is taken into account in the near-field by direct noise simulation without having to perform volume integration since the surface source terms account for noise generated by acoustic sources in the flow field outside of the blade surface but inside the permeable integration surface. In this case the volume source can be considered as having a negligible contribution.

Regarding more complex flows such as the presently simulated flow around the wind turbine blade tip, discrepancies between direct noise simulation and acoustic analogy methods are even more evident due to the larger velocity gradients and non-linear flow features in the near blade region at the tip of the wind turbine blade. Strong velocity gradients are present in the near blade region, in the domain extending one to two chord lengths away from the wind turbine blade tip. When the permeable integration surface is placed sufficiently far from the blade tip, the mean flow can be considered reasonably uniform, and acoustic analogy methods can be applied to provide accurate prediction of aerodynamic noise over long distances from the blade.

Acoustic analogy models are not sufficiently accurate when simulating complex geometries which exhibit strong reflection, such as winglets for future wind turbine applications. The merits of direct noise simulation in the near blade field can be expected to become even more evident for complex geometries due to the consideration of acoustic reflection effects.

A clear advantage of permeable integration surfaces used in accordance with the acoustic analogy methods is that they enable consideration of conveniently placed fictitious surfaces surrounding a body with a complex geometry. The assumption that the integration surface has to coincide with the body surface would render the sound prediction procedure much more difficult for complex blade tip shapes and would not be able to realistically model the acoustic wave propagation process in the vicinity of the body.

Finally, a major disadvantage of the integration of the blade surface pressure fluctuations by the FW-H equation is the fact that it assumes that the blade chord length is much smaller than the wavelength of the noise of interest, the so called compact body assumption. This assumption is clearly violated regarding wind turbine tip noise. The smallest wavelength of interest is 0.03 m, for 10 kHz, while the blade chord length at the tip is approximately 0.2 m. Even though the use of a fictitious permeable integration surface instead of the blade surface does not completely satisfy the compact body assumption, it can be thought that the compact body assumption is partly relaxed with the fictitious integration surface.

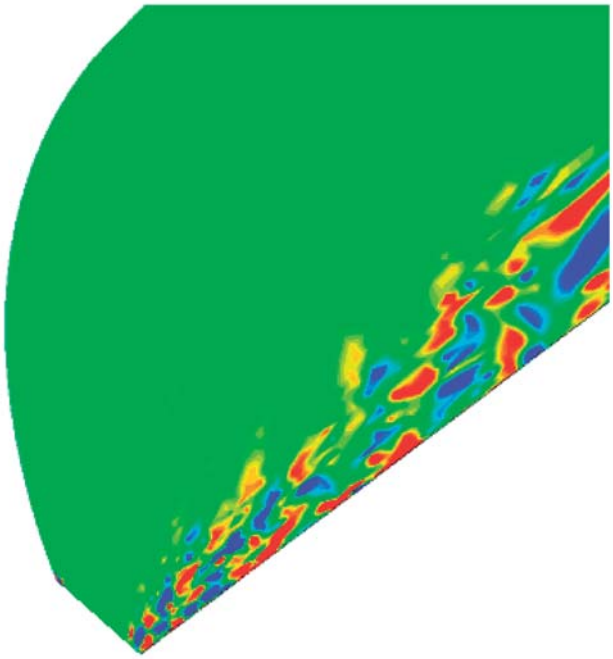

Fig. 21 Surface distribution for actual tip shape (reference point 20 m upstream). Monopole contribution.

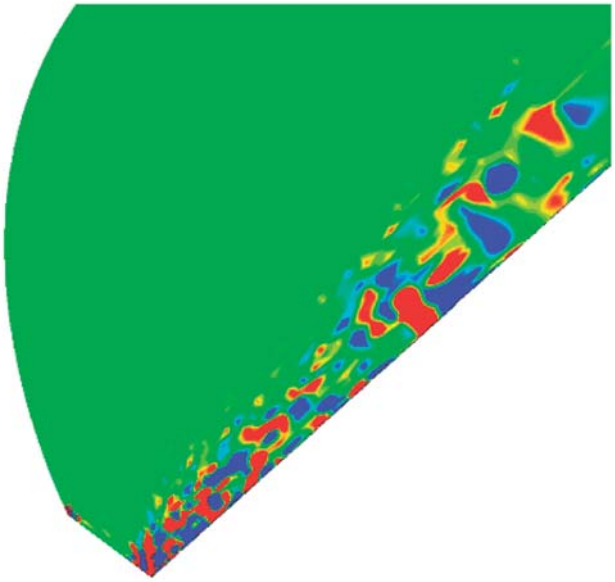

Fig. 22 Surface distribution for actual tip shape (reference point 20 m upstream). Dipole contribution.

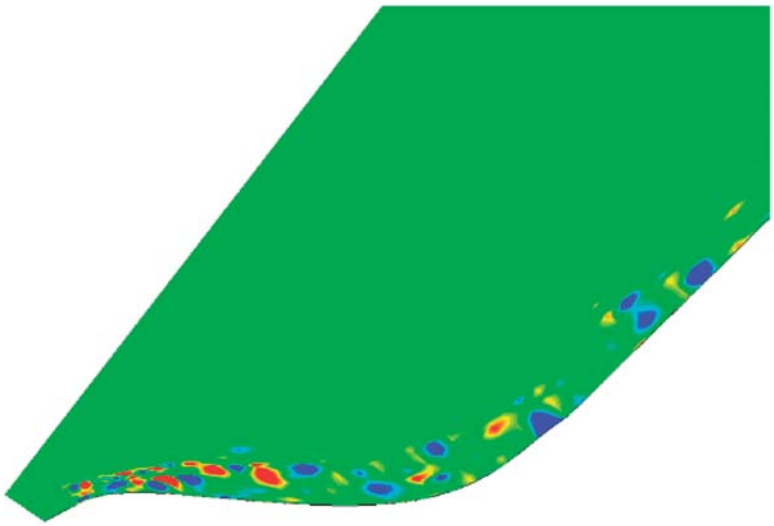

Fig. 23 Surface distribution for ogee tip shape (reference point 20 m upstream). Monopole contribution.

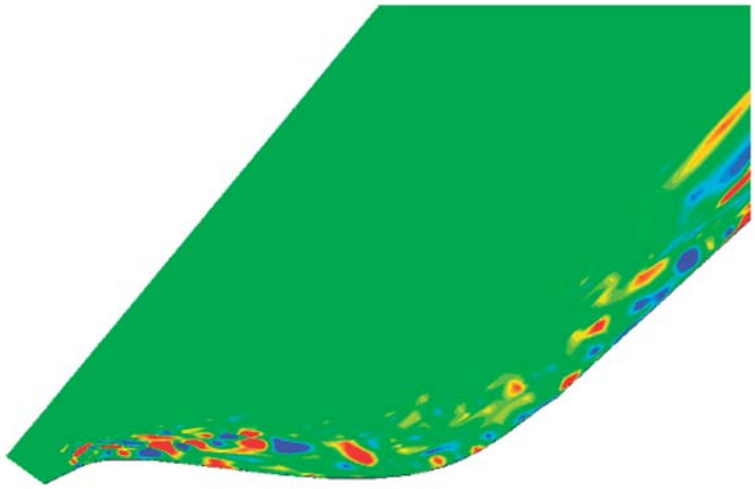

Fig. 24 Surface distribution for ogee tip shape (reference point 20 m upstream). Dipole contribution.

3.9 Effect of blade tip geometry

The physical mechanisms of acoustic wave propagation in the blade tip region are investigated in more detail in order to understand how the blade tip shape affects the tip vortex noise level and why the ogee type tip shape leads to a noise reduction in the high frequency domain.

Figures 21 to 24 show the surface distribution of the monopole and dipole terms of acoustic pressure for the actual and the ogee type tip shapes at the reference point located 20 m upstream of the wind turbine. It can be seen that the actual tip shape exhibits stronger contributions of sound sources along the trailing edge of the wind turbine blade iin the tip region. This can be observed especially for the dipole contribution in Fig. 22, where very intense sound sources are located at the trailing edge at the immediate tip of the blade, most likely due to strong interaction between the shed tip vortex and the blade trailing edge. Concerning the ogee type tip shape, it can be seen that the regions with strong vorticity and sound sources are shifted from the immediate tip towards inner regions, suggesting that the most prominent noise sources are located away from the blade tip, leading to noise reduction for the ogee type tip shape. Strong interaction between the shed tip vortex and the blade trailing edge is minimized due to the curved trailing edge.

The simulation provides new insights into the physical phenomena related to tip vortex formation and tip vortex noise. It allows to investigate the effect of the blade tip

shape on the overall aerodynamic noise radiated by the wind turbine. A better understanding of the physical phenomena of tip vortex noise and a comparison of the level of tip noise emitted by different blade tip shapes will be useful to develop new blade tip designs with reduced noise emission. Initial observations lead to the conclusion that the interaction between the tip vortex shed at the extreme tip of the wind turbine blade and the trailing edge of the wind turbine blade is reduced for the ogee type tip shape due to the curved trailing edge. The trailing edge of the ogee type tip shape is designed so that it avoids interaction with the tip vortex.

4. Conclusion

A computational model for aerodynamic noise prediction that takes into account the true shape of the wind turbine blade geometry was developed. This is an important step towards wind turbine blade design with respect to aerodynamic noise reduction.

The model was applied to the blade tip of WINDMELIII. A direct noise simulation was performed with compressible Large-Eddy Simulation (LES). Acoustic wave propagation was simulated directly from the hydrodynamic field. Far-field noise was predicted using Ffowcs Williams-Hawkings integral method (FW-H).

The far-field broadband noise caused by a rotating wind turbine blade of WINDMELIII type was computed, with particular emphasis on tip vortex noise. The analysis of the pressure fluctuations in the immediate vicinity of the blade showed that the actual tip shape exhibits very high frequency pressure fluctuations that do not appear for the ogee type tip shape. The structure of the tip vortex was shown to be more complex for the actual tip shape. The degree of interaction between the tip vortex and the wind turbine blade trailing edge was reduced for the ogee type tip shape. It was found that the use of an ogee type tip shape can reduce the noise level for frequencies above 3 kHz by up to 5 dB. Overall reduction was found to be 2 dB. Direct noise simulation combined with surface integration on a permeable fictitious surface has the ability to account for accurate acoustic propagation through regions with strong velocity gradients, typically existing in close proximity to the blade surface.

The present study has lead to new insights into acoustic phenomena and physical flow phenomena arising in the wind turbine tip region, phenomena which could not have been obtained by more commonly used Reynolds-averaged Navier-Stokes simulation (RANS) or from empirical equations. A reduction of 2 dB is extremely significant in wind farms and for future large wind turbines with increased tip speed ratio. The design tool developed in this research provides highly accurate far-field noise spectra for arbitrary wind turbine blade geometries. It can contribute towards proposing new ways for designing less noisy wind turbines. The present design tool can be applied to more complex wind turbine blade tip geometries where the merits of direct noise simulation in the blade near-field could become even more noticeable due to the consideration of acoustic reflection effects. Several design recommendations can be drawn from the present simulation results. It would be ideal to design a blade tip shape that reduces the interaction of the turbulent vortex core with the trailing edge and the tip vortex shedding. Noise reduction could be achieved by smoothly cutting away the trailing edge and preventing sharp curves on the leading edge, thus reducing tip vortex-blade interaction.

Acknowledgements

The authors would like to express profound gratitude to the Earth Simulator Center for providing the computational resources for this research. The wind turbine group at the National Institute of Advanced Industrial Science and Technology is gratefully acknowledged for the support of the wind turbine WINDMELIII. One of the authors is also very thankful to the 21st Century COE Program, “Mechanical Systems Innovation”, by the Ministry of Education, Culture, Sports, Science and Technology, for supporting several international conference trips.

References

[1] Burton, T., Sharpe, D., Jenkins, N., Bossanyi, E., Wind Energy Handbook, John Wiley & Sons Ltd, pp.531–533, 2001.

[2] Wagner, S., Bareis, R. and Guidati, G., Wind turbine noise, Springer-Verlag, Berlin. 1996,

[3] Brooks, T. F. and Marcolini, M. A., Airfoil Tip Vortex Formation Noise, *AIAA Journal*, Vol.**24**, No.2, pp.246–252, 1986.

[4] Nii, Y., Takahashi, N., Matsumiya, H., Broadband noise source localization by line microphone array positioned near a wind turbine rotor blade, *The 2001 International Congress and Exhibition on Noise Control Engineering*, The Hague, 2001.

[5] Klug, H., Osten, T., et al., Aerodynamic Noise from Wind Turbines and Rotor Blade Modification, Joule 2 – Project JOU2-CT92-0233, Final Report DEWI-V-950006, 1995.

[6] Matsuo, Y., Numerical Simulation of High speed Turboprop flow (Japanese), Doctoral Thesis, The University of Tokyo, 1988.

[7] Beam, R. M. and Warming, R. F., An Implicit Factored Scheme for the Compressible Navier-Stokes Equations, *AIAA Journal*, Vol.**16**, No.4, pp.393–402, 1978.

[8] Pulliam, T. H. and Chaussee, D. S., A Diagonal Form of

an Implicit Approximate-Factorization Algorithm, *Journal of Computational Physics*, Vol.**39**, pp.347–363, 1981.

[9] Steger, J. L. and Warming, R. F., Flux Vector Splitting of the Inviscid Gasdynamic Equations with Application to Finite-Difference Methods, *Journal of Computational Physics*, Vol.**40**, pp.263–293, 1981.

[10] Obayashi, S., Fujii, K., Computation of three-dimensional viscous transonic flows with the LU factored scheme, *AIAA 85-1510*, pp.192–202, 1985.

[11] Anderson, J. D. Jr., Modern Compressible Flow – with Historical Perspective, Second Edition, McGraw-Hill Publishing Company, 1990.

[12] Piomelli, U., Balaras, E., Wall-layer models for large eddy simulations, *Annual Review Fluid Mechanics*, Vol.**34**, pp.349–374, 2002.

[13] Spalart, P. R, Strategies for turbulence modeling and simulations, *International Journal of Heat and Fluid Flow*, Vol.**21**, pp.252–263, 2000.

[14] Leornard, A., Energy cascade in Large-Eddy Simulations of turbulent fluid flows, *Advances in Geophysics*, Vol.**18A**, pp.237–248, 1974.

[15] Smagorinsky, J., General Circulation Experiments with the Primitive Equations, *Monthly Weather Review*, Vol.**91**, No.3, pp.99–164, 1963.

[16] Van Driest, E. R., On the turbulent flow near a wall, *Journal of Aeronautical Science*, Vol.**23**, p.1007, 1956.

[17] Tam, C. K. W., Webb, J. C., Dispersion-Relation-Preserving Finite Difference Schemes for Computational Acoustics, *Journal of Computational Physics*, Vol.**107**, pp.262–281, 1993.

[18] Piomelli, U., Large-eddy simulation: achievements and challenges, *Progress in Aerospace Sciences*, Vol.**35**, pp.335–362, 1999.

[19] Lighthill, M. J., On Sound Generated Aerodynamically. I: General Theory, *Proceedings of the Royal Society*, Vol.**A221**, pp.564–587, 1952.

[20] Lighthill, M. J., On Sound Generated Aerodynamically. II: Turbulence as a source of sound, *Proceedings of the Royal Society*, Vol.**A222**, pp.1–32, 1954.

[21] Curle, N., The influence of Solid Boundaries upon Aerodynamic Sound, *Proc. Royal Soc.* London, **A231**, pp.505–514, 1955.

[22] Ffowcs Williams, J. E., Hawkings, D. L., Sound Generation by Turbulence and Surfaces in Arbitrary Motion, Phil. Trans. of the Royal Soc. Of London, *A: Mathematical and Physical Sciences*, Vol.**264**, No.1151, pp.321–342, 1969.

[23] Di Francescantonio, P., A New Boundary Integral Formulation for the Prediction of Sound Radiation, *Journal of Sound and Vibration*, Vol.**202**, No.4, pp.491–509, 1997.

[24] Brentner, K. S. and Farassat F., Analytical Comparison of the Acoustic Analogy and Kirchhoff Formulation for Moving Surfaces, *AIAA Journal*, Vol.**36**, No.8, pp.1379–1386, 1998.

[25] Manoha, E., Herrero, C., Sagaut, P., Redonnet, S., Numerical Prediction of Airfoil Aerodynamic Noise, AIAA 2002-2573, 2002.

[26] Aoyama, Y., Parallel Computing by MPI, (Japanese), IBM Japan, 1999.

[27] Druault P., Lardeau S. S, Bonnet J.-P., Coiffet F., Delville J., Lamballais E., Largeau J. F., Perret L., Generation of Three-Dimensional Turbulent Inlet Conditions for Large-Eddy Simulation, *AIAA Journal*, Vol.**42**, No.3, pp.447–456, 2004.

[28] Iida, M., Arakawa, C., Matsumiya, H., Three Dimensional flow Analysis of Horizontal Axis Wind Turbine Blade Using Overset Grid Method, *Proceedings of the 21st EWEC*, Kassel, Germany, 2000.

[29] Powell, A., The Theory of Vortex Sound, *Journal of the Acoustical Society of America*, Vol.**33**, pp.177–195, 1964.

[30] Nii, Y., Matsumiya, H., Kogaki, T., Iida, M., Broadband Noise Sources of an Experimental Wind Turbine Rotor Blade, (Japanese), *Transactions of the Japan Society of Mechanical Engineers*, Part B, Vol.**70**, No.692, pp.99–104, 2004.